Power Allocation for Intelligent Interference Exploitation Aided Physical-Layer Security in OFDM-Based Heterogeneous Cellular Networks

Yuhan Jiang, Yulong Zou, *Senior Member, IEEE*, Haiyan Guo, Jia Zhu, and Jiahao Gu

***Abstract*—In this paper, we consider an orthogonal frequency division multiplexing (OFDM) based heterogeneous cellular network consisting of a macro cell and a small cell, where a macro-cell base station (MBS) and a small-cell base station (SBS) communicate with respective macro-cell user (MU) and small-cell user (SU) with the existence of a common eavesdropper across different OFDM subcarriers. In order to make full use of the mutual interference between MBS and SBS against eavesdropping, an artificially designed signal is emitted at MBS to cancel out the interference received at MU as well as to interfere with the common eavesdropper at each subcarriers. For the purpose of further improving the secrecy performance, a sum secrecy rate (SSR) of OFDM-based heterogeneous cellular networks is maximized by optimizing the power allocation between MBS and SBS across different OFDM subcarriers when the eavesdropper owns the global instantaneous channel state information (ICSI), thus called ICSI based SSR maximization (ICSI-SSRM). As for the case when the ICSI of wiretap channels is unknown, we propose a statistical CSI based SSR maximization (SCSI-SSRM) scheme, where the statistical characteristics of channels from MBS and SBS to eavesdropper are employed to optimally allocate powers of MBS and SBS across different subcarriers under the constraint of MBS's total transmit power. The formulated ICSI-SSRM and SCSI-SSRM problems are all non-convex due to form of the difference between two-convex (D.C.) functions. Thus, we utilize the D.C. approximation approach to respectively convert original optimization problems into convex problems. Moreover, iterative optimal power allocation algorithms for ICSI-SSRM and SCSI-SSRM schemes are also presented to obtain their respective SSR values. Simulation results illustrate that the ICSI-SSRM and SCSI-SSRM algorithms can converge to their optimal values, which confirms the correctness and validation of the proposed algorithms. In addition, numerical results are also given to show that the ICSI-SSRM and SCSI-SSRM schemes outperform conventional power allocation methods in terms of their SSR performance.**

***Index Terms*—Heterogeneous cellular networks, power allocation, interference, physical-layer security.**

Manuscript received June 7, 2019; revised September 10, 2019 and November 25, 2019; accepted January 2, 2020. Date of publication January 14, 2020; date of current version March 12, 2020. This work was supported in part by the National Natural Science Foundation of China under Grants 61631020, 61671253, and 91738201, in part by the Natural Science Foundation of Jiangsu Province under Grant BK20171446, in part by the Key Project of Natural Science Research of Higher Education Institutions of Jiangsu Province under Grant 18KJB510031, in part by the Postgraduate Research & Practice Innovation Program of Jiangsu Province under Grant KYCX19_0892, and in part by the Open Research Foundation of Key Laboratory of Dynamic Cognitive System of Electromagnetic Spectrum Space (Nanjing Univ. Aeronaut. Astronaut.), Ministry of Industry and Information Technology under Grant KF20181910. The review of this article was coordinated by Dr. J. Liu. *(Corresponding author: Yulong Zou.)*

Y. Jiang, Y. Zou, J. Zhu, and J. Gu are with the School of Telecommunications and Information Engineering, Nanjing University of Posts and Telecommunications, Nanjing 210003, China (e-mail: 15262769115@163.com; yulong.zou@njupt.edu.cn; jiazhu@njupt.edu.cn; Q16010125@njupt.edu.cn).

H. Guo is with the School of Telecommunications and Information Engineering, Nanjing University of Posts and Telecommunications, Nanjing 210003, China, and also with the Key Laboratory of Dynamic Cognitive System of Electromagnetic Spectrum Space (Nanjing Univ. Aeronaut. Astronaut.), Ministry of Industry and Information Technology, Nanjing 210003, China (e-mail: guohy@njupt.edu.cn).

Digital Object Identifier 10.1109/TVT.2020.2966637

I. Introduction

NOWADAYS, with the emergence of various wireless communication devices [1], [2], such as mobile phones, tablet computers, smart watches and so on, the demand for radio spectrum resources is increasing explosively. Thus, it is of great importance to improve the spectral efficiency [3]–[5]. Heterogeneous cellular network is considered as an effective means of taking full advantages of radio spectrum resources and boosting the network capacity [6], [7]. Specifically, the spectrum resources can be simultaneously accessed by both the macro-cell user (MU) and small-cell user (SU) in heterogeneous cellular networks to achieve a higher spectral efficiency [8], [9]. Besides, in order to meet the high speed data rates, orthogonal frequency division multiplexing (OFDM) technology has been employed in heterogeneous cellular networks [10], [11]. However, since a macro cell shares the same spectrum resources with a small cell at each subcarriers, a mutual interference among them degrades the performance of OFDM-based heterogeneous cellular networks. Therefore, it is important to investigate power allocation and interference management to control and limit such mutual interferences [12]–[15]. More specifically, in heterogeneous cellular networks, the interference caused by each mobile terminals was controlled below a predefined threshold by designing a stochastic geometry based power allocation mechanism [16]. Later on, for the purpose of degrading the inter-cell interference received at the offloaded users caused by macro-cell base stations (MBSs), the authors of [17] proposed a scheme combing reverse frequency allocation with user association.

Besides, although the opening nature of wireless communications brings a lot of convenience to our lives, it is also vulnerable to eavesdropping attacks. For example, an eavesdropper may overhear the confidential information transmitted over heterogeneous cellular networks [18], [19]. Thus, extensive research efforts have been devoted to defend against eavesdropping and

further enhance the secrecy performance of wireless communications, including beamforming (BF) [20], cooperative relays [21], artificial noise (AN) [22], cooperative jamming [23], [24] and so on. To be specific, in [20], a joint BF and time allocation scheme was proposed to maximize the sum rates of the device-to-device (D2D) users in a time-division duplex D2D cellular network by taking into account the quality-of-service requirement of cognitive users. The secrecy capacity was improved in [21] by employing relay nodes to assist the transmission from source to destination, where outage probability and intercept probability of both single-relay selection and multi-relay selection schemes were analyzed. Additionally, the authors of [22] injected AN signals to confuse the eavesdropper in a multiple-input-single-output (MISO) multicast system with available eavesdropper's statistical channel state information (CSI), and applied BF to guarantee that AN signals would not cause the interference to legitimate users. Moreover, [23] proposed a cooperative jamming scheme to defend against randomly distributed eavesdroppers and designed jammer placement algorithms to obtain the optimal number of jammers. In order to obtain secure transmission in MISO wiretap channels, the authors of [24] jointly utilized the BF, AN and friendly jammering technologies to maximize the secrecy rate, where full CSI and channel distribution information of eavesdropper were considered.

Meanwhile, considerable attentions have been paid to the physical-layer security (PLS) of heterogeneous spectrum-sharing networks [25]–[31]. More specifically, the closed-from expressions of outage probability for D2D communication enabled multi-channel cellular networks were derived in [25]. Moreover, the D2D technology was employed in LTE-Advanced networks to improve energy efficiency, delay, throughput [26] and quality of experience [27] as well as load balancing efficiency [28]. The PLS of a multi-tier heterogeneous cellular network having random distributed base stations, users and eavesdroppers was studied in [29] in terms of connection probability and secrecy probability. Also, the authors of [30] employed friendly jammers and full-duplex users to improve the PLS of heterogeneous spectrum-sharing networks. More recently, the author of [31] proposed a so-called interference-canceled underlay spectrum sharing (IC-USS) scheme to improve the PLS of heterogeneous cellular networks, where an artificial signal was designed and emitted at MBS to cancel out the interference received at MU and to interfere with an eavesdropper. Nevertheless, the ratio of transmit power of the small-cell base station (SBS) to that of the MBS for IC-USS scheme in [31] was fixed to analyze the system overall outage probability and intercept probability as well as secrecy diversity. It is worth mentioning that the transmit power allocation between MBS and SBS can be further optimized to enhance the PLS of heterogeneous cellular networks.

In this paper, for the purpose of enhancing the spectral efficiency, limiting the interference and degrading the eavesdropper, we are motivated to examine an optimization of transmit power allocation between MBS and SBS across different OFDM subcarriers to maximize the sum secrecy rate (SSR) of both macro cell and small cell in an OFDM-based heterogeneous cellular network, where both the instantaneous and statistical CSI of eavesdropper are considered. The differences between this paper and [31] are listed as follows. First, we consider an OFDM based heterogeneous cellular network in our system model, which is more complex than [31], where the allocated power for MBS and SBS was fixed. It is more challenging to perform the optimal power allocation between MBS and SBS across different OFDM subcarriers. Second, this paper takes into account both the instantaneous and statistical CSI of wiretap links to maximize the SSR of OFDM based heterogeneous cellular networks. The main contributions of this paper can be summarized as follows.

- We consider an OFDM based heterogeneous cellular network, where a specially-designed signal is emitted at MBS to cancel out the interference caused by SBS for any OFDM subcarrier. To maximize the SSR of both macro cell and small cell in an OFDM-based heterogeneous cellular network, we propose an instantaneous CSI (ICSI) based SSR maximization (ICSI-SSRM) scheme by optimizing the power allocation between MBS and SBS across different OFDM subcarriers. As for the case when the ICSI of eavesdropper is unknown, a statistical CSI (SCSI) based SSR maximization (SCSI-SSRM) strategy is also analyzed in OFDM based heterogeneous cellular networks.
- Due to the fact that our proposed ICSI-SSRM and SCSI-SSRM problems are non-convex, we firstly apply the difference of two-convex functions (D.C.) approximation method to transform the original problems into convex problems. Then iterative power allocation algorithms are proposed to obtain the corresponding optimal solutions for ICSI-SSRM and SCSI-SSRM schemes.
- Numerical simulations are carried out to show the convergence performance of our proposed iterative ICSI-SSRM and SCSI-SSRM algorithms. It is also shown that proposed ICSI-SSRM and SCSI-SSRM schemes obtain a better secrecy performance than conventional power allocation approaches.

The rest of this paper is organized as follows. In Section II, we describe the system model and formulate ICSI-SSRM and SCSI-SSRM problems in OFDM-based heterogeneous cellular networks. Next, Section III respectively gives the solutions of our formulated ICSI-SSRM and SCSI-SSRM problems and presents corresponding iterative optimal power allocation algorithms, followed by Section IV, where numerical simulation results are given to show the advantage of the proposed ICSI-SSRM and SCSI-SSRM schemes. Finally, a brief summary of our results is provided in Section V.

A list of notations and representations used in this paper is presented in Table I.

II. System Model and Problem Formulation

In this section, we present the system model of an orthogonal frequency division multiplexing (OFDM) based heterogeneous cellular network, where the interference received at macro-cell user (MU) is canceled out at each subcarrier. Then, we formulate instantaneous channel state information (ICSI) based sum secrecy rate maximization (ICSI-SSRM) and statistical channel state information (SCSI) based sum secrecy rate maximization (SCSI-SSRM) schemes in OFDM-based heterogeneous cellular networks.

TABLE I
NOTATIONS AND REPRESENTATIONS

Notations	Representations
$\lvert\cdot\rvert$	Absolute value
$\sqrt{\cdot}$	Square root operation
$(\cdot)^2$	Square operation
$E(\cdot)$	Statistical expectation
$\max(\cdot)$	Maximum value
$\min(\cdot)$	Minimum value
$\mathcal{CN}(0,\sigma^2)$	A complex Gaussian random variable with zero mean and variance σ^2

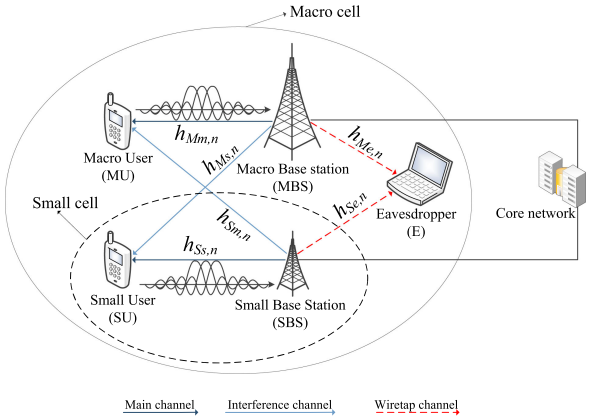

Fig. 1. An OFDM-based heterogeneous cellular network comprised of a macro cell and a small cell in the presence of an eavesdropper.

A. System Model

As shown in Fig. 1, we consider an OFDM-based heterogeneous cellular network consisting of a macro-cell network and a small-cell network. There are N subcarriers in each OFDM symbol. For any OFDM subcarrier, a macro-cell base station (MBS) uses the same spectrum with a small-cell base station (SBS) to communicate with respective macro-cell user (MU) and small-cell user (SU) in the face of a common eavesdropper (E). Each node in this paper is equipped with a single antenna. MBS and SBS are connected to a core network through fiber cable to exchange information. It is noted that the focus of this paper is to maximize the sum secrecy rate (SSR) of both macro cell and small cell by optimizing the power allocation of MBS and SBS across different OFDM subcarriers in heterogeneous cellular networks, considering the instantaneous and statistical channel state information (CSI) of eavesdropper. Our proposed iterative power allocation algorithm can be used for some more complex scenarios. For example, each node in our system model is equipped with multiple antennas. According to [32] and [33], we may consider the use of the transmit antenna selection at MBS and SBS as well as the maximum ratio combining at MU, SU and E along with a similar iterative power allocation algorithm to address the multi-antenna scenarios. Moreover, although only one macro cell and small cell are considered in our system model, it can be extended to a general large-scale heterogeneous cellular network having massive macro cells and small cells with the aid of base station pairing and grouping. In such cases, we divide the whole spectrum into multiple orthogonal sub-bands, which are then allocated to different MBS-SBS pairs [31]. Additionally, we may consider both the large-scale path loss and small-scale Rayleigh fading in modeling wireless channels, and investigate the impact of transmission distances on the SSR performance of our proposed ICSI-SSRM and SCSI-SSRM schemes, which may be considered for our future work.

In order to defend against the interference caused by SBS as well as to interfere with a common eavesdropper, an artificially designed signal $x_{m,n}$ is emitted at MBS on subcarrier n. Thus, the transmit signals of MBS and SBS at the n_{th} subcarrier can be respectively expressed by

$$x_{\mathrm{MBS},n} = \sqrt{P_{M,n} - \bar{P}_{m,n}}x_{M,n} + x_{m,n}, \tag{1}$$

$$x_{\mathrm{SBS},n} = \sqrt{P_{S,n}}w_{S,n}x_{S,n}, \tag{2}$$

where $P_{M,n}$ denotes the sum of the transmit power of $x_{M,n}$ and $x_{m,n}$, and $\bar{P}_{m,n}$ is the average transmit power of artificially designed signal $x_{m,n}$ on subcarrier n. The remaining power $P_{M,n} - \bar{P}_{m,n}$ is used to transmit signal $x_{M,n}$ at the n_{th} subcarrier, where $P_{M,n} \geq 0$ and $0 \leq \bar{P}_{m,n} \leq P_{M,n}$. Note that the average transmit power of $x_{m,n}$ is used in (1) instead of the instantaneous power, which is due to the fact that the instantaneous transmit power $P_{m,n}$ may exceed the total transmit power of $P_{M,n}$, and further result in that the transmit power of MBS for the desired signal $x_{M,n}$ is less than zero [31]. $x_{S,n}$ and $P_{S,n}$ are the transmit signal and power of SBS at the n_{th} subcarrier, $w_{S,n}$ is a weight coefficient of the SBS's signal on subcarrier n. Hence, the received signal at MU on subcarrier n can be given by

$$\begin{aligned} y_{m,n} &= h_{Mm,n}\left(\sqrt{P_{M,n} - \bar{P}_{m,n}}x_{M,n} + x_{m,n}\right) \\ &\quad + h_{Sm,n}\sqrt{P_{S,n}}w_{S,n}x_{S,n} + n_{m,n} \\ &= \sqrt{P_{M,n} - \bar{P}_{m,n}}h_{Mm,n}x_{M,n} \\ &\quad + \left(h_{Mm,n}x_{m,n} + \sqrt{P_{S,n}}h_{Sm,n}w_{S,n}x_{S,n}\right) + n_{m,n}, \end{aligned} \tag{3}$$

where $h_{Mm,n}$ and $h_{Sm,n}$ represent the fading coefficients of MBS-MU and SBS-MU channel at the n_{th} subcarrier, respectively. $n_{m,n} \sim \mathcal{CN}(0, \sigma_{m,n}^2)$ is additive white Gaussian noise (AWGN) at MU on subcarrier n. For the purpose of cancelling out the interference at MU caused by SBS, the artificially designed signal $x_{m,n}$ and the weight coefficient $w_{S,n}$ at the n_{th} subcarrier should satisfy

$$h_{Mm,n}x_{m,n} + \sqrt{P_{S,n}}h_{Sm,n}w_{S,n}x_{S,n} = 0, \tag{4}$$

due to the fact that MBS and SBS are connected by a core network, so that $x_{S,n}$ and $P_{S,n}$ can be easily obtained at MBS. What's more, MBS can acquire the CSI of $h_{Sm,n}$ and $h_{Mm,n}$ through various channel estimation methods [34]. Thus, we can achieve a solution of the artificially designed signal $x_{m,n}$ and the weight coefficient $w_{S,n}$ at the n_{th} subcarrier as

$$\begin{aligned} [x_{m,n}, w_{S,n}] &= \frac{1}{\sigma_{Mm,n}} \\ &\times \left[-\sqrt{P_{S,n}}\,|h_{Sm,n}|e^{-j\theta_{Mm,n}}x_{S,n}, |h_{Mm,n}|e^{-j\theta_{Sm,n}}\right], \end{aligned} \tag{5}$$

where $\sigma^2_{Mm,n} = E(|h_{Mm,n}|^2)$ denotes the channel variance of MBS-MU on subcarrier n. $\theta_{Mm,n}$ and $\theta_{Sm,n}$ are the channel phases of MBS-MU and SBS-MU at the n_{th} subcarrier. Then, the instantaneous and average transmit powers of $x_{m,n}$ on subcarrier n can be given by

$$\left[P_{m,n}, \bar{P}_{m,n}\right] = \left[\frac{|h_{Sm,n}|^2}{\sigma^2_{Mm,n}} P_{S,n}, \frac{\sigma^2_{Sm,n}}{\sigma^2_{Mm,n}} P_{S,n}\right], \quad (6)$$

where $\sigma^2_{Sm,n} = E(|h_{Sm,n}|^2)$ is the variance of channel from SBS to MU at the n_{th} subcarrier. According to the range of $0 \le \bar{P}_{m,n} \le P_{M,n}$, we can achieve

$$0 \le \frac{\sigma^2_{Sm,n}}{\sigma^2_{Mm,n}} P_{S,n} \le P_{M,n}. \quad (7)$$

Substituting (4) into (3), we can express the received signal at MU on subcarrier n as

$$y_{m,n} = \sqrt{P_{M,n} - \bar{P}_{m,n}} h_{Mm,n} x_{M,n} + n_{m,n}. \quad (8)$$

According to the Shannon's capacity formula, the channel capacity of MBS-MU channel at the n_{th} subcarrier can be written as

$$C_{Mm,n} = \log_2(1 + \gamma_{Mm,n}), \quad (9)$$

where

$$\gamma_{Mm,n} = \frac{\left(P_{M,n} - \sigma^2_{Sm,n} P_{S,n}/\sigma^2_{Mm,n}\right) |h_{Mm,n}|^2}{\sigma^2_{m,n}}. \quad (10)$$

Similarly, the received signal of SU on subcarrier n is given by

$$y_{s,n} = h_{Ms,n}\left(\sqrt{P_{M,n} - \bar{P}_{m,n}} x_{M,n} + x_{m,n}\right) + h_{Ss,n}\sqrt{P_{S,n}} w_{S,n} x_{S,n} + n_{s,n}, \quad (11)$$

where $h_{Ss,n}$ and $h_{Ms,n}$ represent the fading coefficients of SBS-SU and MBS-SU channel at the n_{th} subcarrier, respectively, and $n_{s,n} \sim \mathcal{CN}(0, \sigma^2_{s,n})$ is the AWGN received at SU on subcarrier n. Thus, the channel capacity of SBS-SU channel at the n_{th} subcarrier can be expressed by

$$C_{Ss,n} = \log_2\left(1 + \gamma_{Ss,n}\right), \quad (12)$$

where

$$\gamma_{Ss,n} = \frac{P_{S,n} |h_{Ss,n}|^2 |h_{Mm,n}|^2 \Big/ \sigma^2_{Mm,n}}{\left[P_{M,n} + (|h_{Sm,n}|^2 - \sigma^2_{Sm,n}) P_{S,n} \Big/ \sigma^2_{Mm,n}\right] |h_{Ms,n}|^2 + \sigma^2_{s,n}}. \quad (13)$$

B. ICSI-SSRM Scheme

In this section, we consider an ICSI-SSRM scheme, where the ICSI of wiretap links is assumed to be known. According to [35] and [36], we can exploit the channel estimation technologies to achieve the ICSI of an active eavesdropper. For example, the ICSI of a legitimate user can be obtained through some channel estimation methods. However, the legitimate user may be hacked by a Trojan horse and then becomes an eavesdropper. In this case, the ICSI of such an eavesdropper is the ICSI of a compromised legitimate user. Thus, the received signal at eavesdropper on subcarrier n can be given by

$$y_{e,n} = h_{Me,n}\left(\sqrt{P_{M,n} - \bar{P}_{m,n}} x_{M,n} + x_{m,n}\right) + h_{Se,n}\sqrt{P_{S,n}} w_{S,n} x_{S,n} + n_{e,n}, \quad (14)$$

where $h_{Me,n}$ and $h_{Se,n}$ are the fading coefficients of MBS-E and SBS-E channel at the n_{th} subcarrier, respectively, and $n_{e,n} \sim \mathcal{CN}(0, \sigma^2_{e,n})$ is the AWGN at E on subcarrier n.

Indeed, the eavesdropper may achieve more useful information to perform successive interference cancellation (SIC) [37] to sequentially decode its received signal as given by (14). Meanwhile, the SIC can be also used at SU to obtain a better performance for the legitimate link. Overall speaking, no obvious secrecy benefits are expected by applying the SIC at both E and SU. It is of interest to investigate the impact of SIC on the secrecy performance of SSRM schemes, which is considered for further work. Then, we can write the channel capacity of MBS-E channel at the n_{th} subcarrier as

$$C_{Me,n} = \log_2\left(1 + \gamma_{Me,n}\right), \quad (15)$$

where

$$\gamma_{Me,n} = \frac{\left(P_{M,n} - \sigma^2_{Sm,n} P_{S,n} / \sigma^2_{Mm,n}\right) |h_{Me,n}|^2}{P_{S,n}\left(|h_{Mm,n}|^2 |h_{Se,n}|^2 + |h_{Sm,n}|^2 |h_{Me,n}|^2\right) \Big/ \sigma^2_{Mm,n} + \sigma^2_{e,n}}. \quad (16)$$

Meanwhile, the channel capacity of SBS-E channel on subcarrier n can be given by

$$C_{Se,n} = \log_2(1 + \gamma_{Se,n}), \quad (17)$$

where

$$\gamma_{Se,n} = \frac{P_{S,n} |h_{Se,n}|^2 |h_{Mm,n}|^2 \Big/ \sigma^2_{Mm,n}}{\left[P_{M,n} + \left(|h_{Sm,n}|^2 - \sigma^2_{Sm,n}\right) P_{S,n} \Big/ \sigma^2_{Mm,n}\right] |h_{Me,n}|^2 + \sigma^2_{e,n}}. \quad (18)$$

The ICSI-SSRM problem can be formulated as

$$\max_{P_{M,n}, P_{S,n}} \sum_{n=1}^{N} C_{Mm,n} - C_{Me,n} + C_{Ss,n} - C_{Se,n}$$

$$\text{s.t.} \quad C1: 0 \le \frac{\sigma^2_{Sm,n}}{\sigma^2_{Mm,n}} P_{S,n} \le P_{M,n}$$

$$C2: \sum_{n=1}^{N} P_{M,n} = P_M^{tot}, \quad (19)$$

where P_M^{tot} is total transmit power of MBS. By substituting (10), (13), (16) and (18) into (19), the optimization problem can be simplified as

$$\max_{P_{M,n},P_{S,n}} \sum_{n=1}^{N} f_1(P_{M,n},P_{S,n}) - f_2(P_{M,n},P_{S,n}) \quad \text{s.t.} \quad C1-C2, \tag{20}$$

where $f_1(P_{M,n},P_{S,n})$ and $f_2(P_{M,n},P_{S,n})$ are presented at (21) and (22) shown at the bottom of this page, respectively.

C. SCSI-SSRM Scheme

For the case that the ICSI of eavesdropper is unavailable, we propose the eavesdropper's SCSI based SSRM scheme (denoted by SCSI-SSRM scheme for short) in this section. We assume that the fading coefficients of MBS-E and SBS-E channels at the n_{th} subcarrier are independent complex Gaussian random variables with zero mean and variances $\sigma^2_{Me,n}$ and $\sigma^2_{Se,n}$, respectively, i.e., $h_{Me,n} \sim \mathcal{CN}(0,\sigma^2_{Me,n})$ and $h_{Se,n} \sim \mathcal{CN}(0,\sigma^2_{Se,n})$. Thus, we express the SCSI-SEEM problem as

$$\max_{P_{M,n},P_{S,n}} \sum_{n=1}^{N} \mathrm{E}\left[C_{Mm,n} - C_{Me,n} + C_{Ss,n} - C_{Se,n}\right] \quad \text{s.t.} \quad C1-C2, \tag{23}$$

Then, we focus on solving the following optimization problem, that is

$$\max_{P_{M,n},P_{S,n}} \sum_{n=1}^{N} C_{Mm,n} + C_{Ss,n} - \mathrm{E}[C_{Me,n}] - \mathrm{E}[C_{Se,n}] \quad \text{s.t.} \quad C1-C2, \tag{24}$$

where

$$\mathrm{E}\left[C_{Me,n}\right] = \log_2\left[1+\mathrm{E}(\gamma_{Me,n})\right] = \log_2 \times\left[1+\frac{(P_{M,n}-\sigma^2_{Sm,n}P_{S,n}/\sigma^2_{Mm,n})\sigma^2_{Me,n}}{P_{S,n}(|h_{Mm,n}|^2\sigma^2_{Se,n}+|h_{Sm,n}|^2\sigma^2_{Me,n})/\sigma^2_{Mm,n}+\sigma^2_{e,n}}\right], \tag{25}$$

and

$$\mathrm{E}\left[C_{Se,n}\right] = \log_2\left[1+\mathrm{E}\left(\gamma_{Se,n}\right)\right] = \log_2 \times\left[1+\frac{P_{S,n}\sigma^2_{Se,n}|h_{Mm,n}|^2/\sigma^2_{Mm,n}}{\left[P_{M,n}+\left(|h_{Sm,n}|^2-\sigma^2_{Sm,n}\right)P_{S,n}/\sigma^2_{Mm,n}\right]\sigma^2_{Me,n}+\sigma^2_{e,n}}\right]. \tag{26}$$

More details are given in Appendix A.

Substituting (10), (13), (25) and (26) into (24), we have

$$\max_{P_{M,n},P_{S,n}} \sum_{n=1}^{N} g_1(P_{M,n},P_{S,n}) - g_2(P_{M,n},P_{S,n}) \quad \text{s.t.} \quad C1-C2, \tag{27}$$

where $g_1(P_{M,n},P_{S,n})$ and $g_2(P_{M,n},P_{S,n})$ are given at (28) and (29) shown at the bottom of the next page, respectively.

Lemma: The object functions of optimization problems (20) and (27) are non-convex.

Proof: Please see Appendix B. ■

III. Solution of the Optimization Problem

In this section, we first present the methods to solve the ICSI-SSRM and SCSI-SSRM problems. Afterwards, their corresponding iterative optimal power allocation algorithms are proposed. Next, we analyze the overall computational complexity of the proposed ICSI-SSRM and SCSI-SSRM algorithms. Finally, we give the convergence proof of the iterative processes.

A. Solution of the ICSI-SSRM Scheme

This subsection introduces the method to solve the non-convex ICSI-SSRM problem. Since the optimization problem (20) is a form of the difference between two-convex (D.C.) functions, we apply D.C. approximation method [38] to approximate $f_2(P_{M,n},P_{S,n})$ into a linear function. Then, letting $f_2(\tilde{P}_{M,n},\tilde{P}_{S,n})$ is a feasible solution of $f_2(P_{M,n},P_{S,n})$ and according to the first-order Taylor series expansion of

$$\begin{aligned} f_1(P_{M,n},P_{S,n}) = {} & \log_2\left[1+\frac{\left(P_{M,n}-\sigma^2_{Sm,n}P_{S,n}/\sigma^2_{Mm,n}\right)|h_{Mm,n}|^2}{\sigma^2_{m,n}}\right] + \log_2\left[\frac{P_{S,n}(|h_{Se,n}|^2|h_{Mm,n}|^2+|h_{Me,n}|^2|h_{Sm,n}|^2)}{\sigma^2_{Mm,n}}+\sigma^2_{e,n}\right] \\ & + \log_2\left[P_{M,n}|h_{Ms,n}|^2+\frac{P_{S,n}\left(|h_{Ss,n}|^2|h_{Mm,n}|^2+|h_{Ms,n}|^2|h_{Sm,n}|^2-|h_{Ms,n}|^2\sigma^2_{Sm,n}\right)}{\sigma^2_{Mm,n}}+\sigma^2_{s,n}\right] \\ & + \log_2\left[P_{M,n}|h_{Me,n}|^2+\frac{P_{S,n}|h_{Me,n}|^2\left(|h_{Sm,n}|^2-\sigma^2_{Sm,n}\right)}{\sigma^2_{Mm,n}}+\sigma^2_{e,n}\right] \end{aligned} \tag{21}$$

$$\begin{aligned} f_2(P_{M,n},P_{S,n}) = {} & 2\log_2\left[P_{M,n}|h_{Me,n}|^2+\frac{P_{S,n}\left(|h_{Se,n}|^2|h_{Mm,n}|^2+|h_{Me,n}|^2|h_{Sm,n}|^2-|h_{Me,n}|^2\sigma^2_{Sm,n}\right)}{\sigma^2_{Mm,n}}+\sigma^2_{e,n}\right] \\ & + \log_2\left[P_{M,n}|h_{Ms,n}|^2+\frac{P_{S,n}|h_{Ms,n}|^2\left(|h_{Sm,n}|^2-\sigma^2_{Sm,n}\right)}{\sigma^2_{Mm,n}}+\sigma^2_{s,n}\right] \end{aligned} \tag{22}$$

Algorithm 1: Iterative Optimal Power Allocation Algorithm for ICSI-SSRM Scheme.

1: **Initialization**: $k_{\max}$, ε, $(P^0_{M,n}, P^0_{S,n}) = (0,0)$, $f^0 = 0$ and $k = 0$.
2: **Repeat**:
3: Solve (32) with $(P^k_{M,n}, P^k_{S,n})$ to obtain the optimal solution.
4: Update $f^{k+1} = \sum_{n=1}^{N} f_1(P^{k+1}_{M,n}, P^{k+1}_{S,n}) - f_2(P^{k+1}_{M,n}, P^{k+1}_{S,n})$.
5: $k = k + 1$.
6: **Until**: $|f^k - f^{k-1}| \le \varepsilon$ or $k \ge k_{\max}$
7: **Output**: $P^*_{M,n} = P^k_{M,n}$ and $P^*_{S,n} = P^k_{S,n}$.

$f_2(P_{M,n}, P_{S,n})$, we can achieve (30). Combining the problem (20) and the formula (30) shown at the bottom of this page, we can obtain an approximate optimization problem (31) shown at the bottom of the next page. Thus, assuming that $(\tilde{P}^k_{M,n}, \tilde{P}^k_{S,n})$ and $(\tilde{P}^{k+1}_{M,n}, \tilde{P}^{k+1}_{S,n})$ are the optimal solutions to (31) at iterations k and $k+1$, respectively, the problem (20) can be solved through the iterative procedure (32) shown at the bottom of the next page. Afterwards, one can observe that (31) is convex. Therefore, it is simple and straightforward to solve the problem (31) by using existing convex software tools, e.g., CVX [39].

Moreover, an iterative power allocation algorithm is presented in Algorithm 1 to achieve optimal solutions of our formulated ICSI-SSRM problem. Based on the given value $(P^k_{M,n}, P^k_{S,n})$, we solve problem (32) to obtain the optimal power allocation solution $(P^{k+1}_{M,n}, P^{k+1}_{S,n})$. When all the updated data nearly keeps unchanged or the number of iterations approaches to the maximum value, the iteration stops; otherwise, another round of iteration starts. What's more, the computational complexity of the proposed ICSI-SSRM scheme depends on the number of iterations, variable size and the number of constraints. Given the convergence tolerance ε, we can write the iterations excluding convex programming as $o(\log(f^{up}/\varepsilon))$ wherein

$$f^{up} = \frac{P^{tot}_M \max\left(|h_{Mm,n}|^2\right)}{\min\left(\sigma^2_{m,n}\right)\ln 2} + \frac{P^{tot}_S \max\left(|h_{Ss,n}|^2|h_{Mm,n}|^2\right)}{\min\left(\sigma^2_{s,n}\sigma^2_{Mm,n}\right)\ln 2}. \tag{33}$$

There are $2N$ scalar variables in problem (32), which needs at most $o((2N)^{3.5}\log(1/\varepsilon))$ calculations [40]. Therefore, the overall computational complexity of the proposed ICSI-SSRM scheme [41] can be roughly given by

$$o\left((2N)^{3.5}\log(f^{up}/\varepsilon)\log(1/\varepsilon)\right). \tag{34}$$

B. Solution of the SCSI-SSRM Scheme

In this subsection, we obtain the optimal solutions of the SCSI-SSRM problem. Similar as the ICSI-SSRM problem, denoting $(\hat{P}_{M,n}, \hat{P}_{S,n})$ is a feasible solution of optimization problem (27), the D.C. approximation method [38] is exploited to transform the SCSI-SSRM problem into a convex one (35), which can be solved by CVX [39]. Thus, assuming that $(\hat{P}^k_{M,n}, \hat{P}^k_{S,n})$ and $(\hat{P}^{k+1}_{M,n}, \hat{P}^{k+1}_{S,n})$ are optimal solutions of (35) shown at the bottom of the next page, we are able to achieve the optimal solutions of (27) through the following iterative

$$\begin{aligned} g_1(P_{M,n}, P_{S,n}) = {} & \log_2\left[1 + \frac{(P_{M,n} - \sigma^2_{Sm,n}P_{S,n}/\sigma^2_{Mm,n})|h_{Mm,n}|^2}{\sigma^2_{m,n}}\right] + \log_2\left[\frac{P_{S,n}(\sigma^2_{Se,n}|h_{Mm,n}|^2 + \sigma^2_{Me,n}|h_{Sm,n}|^2)}{\sigma^2_{Mm,n}} + \sigma^2_{e,n}\right] \\ & + \log_2\left[P_{M,n}|h_{Ms,n}|^2 + \frac{P_{S,n}(|h_{Ss,n}|^2|h_{Mm,n}|^2 + |h_{Ms,n}|^2|h_{Sm,n}|^2 - |h_{Ms,n}|^2\sigma^2_{Sm,n})}{\sigma^2_{Mm,n}} + \sigma^2_{s,n}\right] \\ & + \log_2\left[P_{M,n}\sigma^2_{Me,n} + \frac{P_{S,n}\sigma^2_{Me,n}(|h_{Sm,n}|^2 - \sigma^2_{Sm,n})}{\sigma^2_{Mm,n}} + \sigma^2_{e,n}\right] \end{aligned} \tag{28}$$

$$\begin{aligned} g_2(P_{M,n}, P_{S,n}) = {} & 2\log_2\left[P_{M,n}\sigma^2_{Me,n} + \frac{P_{S,n}\left(\sigma^2_{Se,n}|h_{Mm,n}|^2 + \sigma^2_{Me,n}|h_{Sm,n}|^2 - \sigma^2_{Me,n}\sigma^2_{Sm,n}\right)}{\sigma^2_{Mm,n}} + \sigma^2_{e,n}\right] \\ & + \log_2\left[P_{M,n}|h_{Ms,n}|^2 + \frac{P_{S,n}|h_{Ms,n}|^2\left(|h_{Sm,n}|^2 - \sigma^2_{Sm,n}\right)}{\sigma^2_{Mm,n}} + \sigma^2_{s,n}\right] \end{aligned} \tag{29}$$

$$\begin{aligned} f_2(P_{M,n}, P_{S,n}) \le {} & f_2(\tilde{P}_{M,n}, \tilde{P}_{S,n}) + \frac{(P_{M,n} - \tilde{P}_{M,n})|h_{Ms,n}|^2 + (P_{S,n} - \tilde{P}_{S,n})|h_{Ms,n}|^2(|h_{Sm,n}|^2 - \sigma^2_{Sm,n})/\sigma^2_{Mm,n}}{[\tilde{P}_{M,n}|h_{Ms,n}|^2 + \tilde{P}_{S,n}|h_{Ms,n}|^2(|h_{Sm,n}|^2 - \sigma^2_{Sm,n})/\sigma^2_{Mm,n} + \sigma^2_{s,n}]\ln 2} \\ & + \frac{2[(P_{M,n} - \tilde{P}_{M,n})|h_{Me,n}|^2 + (P_{S,n} - \tilde{P}_{S,n})(|h_{Se,n}|^2|h_{Mm,n}|^2 + |h_{Me,n}|^2|h_{Sm,n}|^2 - |h_{Me,n}|^2\sigma^2_{Sm,n})/\sigma^2_{Mm,n}]}{[\tilde{P}_{M,n}|h_{Me,n}|^2 + \tilde{P}_{S,n}(|h_{Se,n}|^2|h_{Mm,n}|^2 + |h_{Me,n}|^2|h_{Sm,n}|^2 - |h_{Me,n}|^2\sigma^2_{Sm,n})/\sigma^2_{Mm,n} + \sigma^2_{e,n}]\ln 2} \end{aligned} \tag{30}$$

Algorithm 2: Iterative Optimal Power Allocation Algorithm for SCSI-SSRM Scheme.

1: **Initialization**: $k_{\max}$, ε, $(P^0_{M,n}, P^0_{S,n}) = (0,0)$, $g^0 = 0$ and $k = 0$.
2: **Repeat**:
3: Solve (36) with $(P^k_{M,n}, P^k_{S,n})$ to obtain the optimal solution.
4: Update $g^{k+1} = \sum_{n=1}^{N} g_1(P^{k+1}_{M,n}, P^{k+1}_{S,n}) - g_2(P^{k+1}_{M,n}, P^{k+1}_{S,n})$.
5: $k = k + 1$.
6: **Until**: $|g^k - g^{k-1}| \le \varepsilon$ or $k \ge k_{\max}$
7: **Output**: $P^*_{M,n} = P^k_{M,n}$ and $P^*_{S,n} = P^k_{S,n}$.

procedure (36) shown at the bottom of the next page. Then, we present the iterative optimal power allocation algorithm for SCSI-SSRM scheme in Algorithm 2.

Finally, following [41], we roughly express the overall computational complexity of the proposed SCSI-SSRM scheme as

$$o\left((2N)^{3.5}\log(g^{up}/\varepsilon)\log(1/\varepsilon)\right), \tag{37}$$

where

$$g^{up} = \frac{P^{tot}_M \max\left(|h_{Mm,n}|^2\right)}{\min\left(\sigma^2_{m,n}\right)\ln 2} + \frac{P^{tot}_S \max\left(|h_{Ss,n}|^2|h_{Mm,n}|^2\right)}{\min\left(\sigma^2_{s,n}\sigma^2_{Mm,n}\right)\ln 2}. \tag{38}$$

Proof: Please see Appendix C for the convergence proof of the iterative processes. ■

IV. Simulation Results

In this section, we present numerical simulations to evaluate the secrecy performances of the proposed ICSI-SSRM and SCSI-SSRM schemes. In our simulations, all channels between two nodes are modelled as Rayleigh fading. Also, we consider $\mathrm{E}(|h_{Ss,n}|^2) = 1$, $\mathrm{E}(|h_{Ms,n}|^2) = 0.1$, $\mathrm{E}(|h_{Sm,n}|^2) = \sigma^2_{Sm,n} = 0.1$, $\mathrm{E}(|h_{Mm,n}|^2) = \sigma^2_{Mm,n} = 1$, $\mathrm{E}(|h_{Me,n}|^2) = \sigma^2_{Me,n} = 1$, $\mathrm{E}(|h_{Se,n}|^2) = \sigma^2_{Se,n} = 1$ and $\sigma^2_{m,n} = \sigma^2_{s,n} = \sigma^2_{e,n} = 0$ dBm.

Fig. 2 shows the convergence behaviour of the proposed ICSI-SSRM and SCSI-SSRM algorithms versus the number of iterations with $N = 10$ and $P^{tot}_M = 25$ dBm. It can be observed that as the number of iterations increases, the sum secrecy rates of both ICSI-SSRM and SCSI-SSRM schemes first increase, and then converge to their corresponding secrecy rate floors. This verifies that the proposed

$$\max_{P_{M,n},P_{S,n}} \sum_{n=1}^{N} f_1(P_{M,n},P_{S,n}) - f_2\big(\tilde{P}_{M,n},\tilde{P}_{S,n}\big) - \frac{\big(P_{M,n}-\tilde{P}_{M,n}\big)|h_{Ms,n}|^2 + \big(P_{S,n}-\tilde{P}_{S,n}\big)|h_{Ms,n}|^2\big(|h_{Sm,n}|^2-\sigma^2_{Sm,n}\big)/\sigma^2_{Mm,n}}{\big[\tilde{P}_{M,n}|h_{Ms,n}|^2+\tilde{P}_{S,n}|h_{Ms,n}|^2(|h_{Sm,n}|^2-\sigma^2_{Sm,n})/\sigma^2_{Mm,n}+\sigma^2_{s,n}\big]\ln 2}$$
$$- \frac{2[(P_{M,n}-\tilde{P}_{M,n})|h_{Me,n}|^2 + (P_{S,n}-\tilde{P}_{S,n})(|h_{Se,n}|^2|h_{Mm,n}|^2 + |h_{Me,n}|^2|h_{Sm,n}|^2 - |h_{Me,n}|^2\sigma^2_{Sm,n})/\sigma^2_{Mm,n}]}{\left[\tilde{P}_{M,n}|h_{Me,n}|^2 + \tilde{P}_{S,n}(|h_{Se,n}|^2|h_{Mm,n}|^2 + |h_{Me,n}|^2|h_{Sm,n}|^2 - |h_{Me,n}|^2\sigma^2_{Sm,n})/\sigma^2_{Mm,n} + \sigma^2_{e,n}\right]\ln 2}$$
$$\text{s.t.} \quad C1 - C2 \tag{31}$$

$$(\tilde{P}^{k+1}_{M,n}, \tilde{P}^{k+1}_{S,n}) =$$
$$\arg\max_{P_{M,n},P_{S,n}} \sum_{n=1}^{N} f_1\big(P_{M,n},P_{S,n}\big) - f_2(\tilde{P}^k_{M,n},\tilde{P}^k_{S,n}) - \frac{\big(P_{M,n}-\tilde{P}^k_{M,n}\big)|h_{Ms,n}|^2 + \big(P_{S,n}-\tilde{P}^k_{S,n}\big)|h_{Ms,n}|^2\big(|h_{Sm,n}|^2-\sigma^2_{Sm,n}\big)/\sigma^2_{Mm,n}}{[\tilde{P}^k_{M,n}|h_{Ms,n}|^2+\tilde{P}^k_{S,n}|h_{Ms,n}|^2(|h_{Sm,n}|^2-\sigma^2_{Sm,n})/\sigma^2_{Mm,n}+\sigma^2_{s,n}]\ln 2}$$
$$- \frac{2\Big[\big(P_{M,n}-\tilde{P}^k_{M,n}\big)|h_{Me,n}|^2 + \big(P_{S,n}-\tilde{P}^k_{S,n}\big)\big(|h_{Se,n}|^2|h_{Mm,n}|^2 + |h_{Me,n}|^2|h_{Sm,n}|^2 - |h_{Me,n}|^2\sigma^2_{Sm,n}\big)/\sigma^2_{Mm,n}\Big]}{\left[\tilde{P}^k_{M,n}|h_{Me,n}|^2 + \tilde{P}^k_{S,n}(|h_{Se,n}|^2|h_{Mm,n}|^2 + |h_{Me,n}|^2|h_{Sm,n}|^2 - |h_{Me,n}|^2\sigma^2_{Sm,n})/\sigma^2_{Mm,n} + \sigma^2_{e,n}\right]\ln 2}$$
$$\text{s.t.} \quad C1 - C2 \tag{32}$$

$$\max_{P_{M,n},P_{S,n}} \sum_{n=1}^{N} g_1\big(P_{M,n},P_{S,n}\big) - g_2\big(\hat{P}_{M,n},\hat{P}_{S,n}\big) - \frac{\big(P_{M,n}-\hat{P}_{M,n}\big)|h_{Ms,n}|^2 + (P_{S,n}-\hat{P}_{S,n})|h_{Ms,n}|^2\big(|h_{Sm,n}|^2-\sigma^2_{Sm,n}\big)/\sigma^2_{Mm,n}}{\left[\hat{P}_{M,n}|h_{Ms,n}|^2 + \hat{P}_{S,n}|h_{Ms,n}|^2(|h_{Sm,n}|^2 - \sigma^2_{Sm,n})/\sigma^2_{Mm,n} + \sigma^2_{s,n}\right]\ln 2}$$
$$- \frac{2\left[(P_{M,n} - \hat{P}_{M,n})\sigma^2_{Me,n} + (P_{S,n} - \hat{P}_{S,n})(\sigma^2_{Se,n}|h_{Mm,n}|^2 + \sigma^2_{Me,n}|h_{Sm,n}|^2 - \sigma^2_{Me,n}\sigma^2_{Sm,n})/\sigma^2_{Mm,n}\right]}{\left[\hat{P}_{M,n}\sigma^2_{Me,n} + \hat{P}_{S,n}\big(\sigma^2_{Se,n}|h_{Mm,n}|^2 + \sigma^2_{Me,n}|h_{Sm,n}|^2 - \sigma^2_{Me,n}\sigma^2_{Sm,n}\big)/\sigma^2_{Mm,n} + \sigma^2_{e,n}\right]\ln 2}$$
$$\text{s.t.} \quad C1 - C2 \tag{35}$$

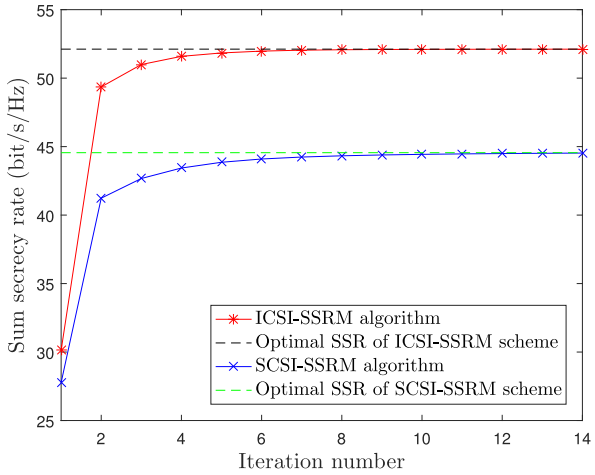

Fig. 2. Covergence behaviour of the proposed ICSI-SSRM and SCSI-SSRM algorithms versus the number of iterations with $N = 10$ and $P_M^{tot} = 25$ dBm.

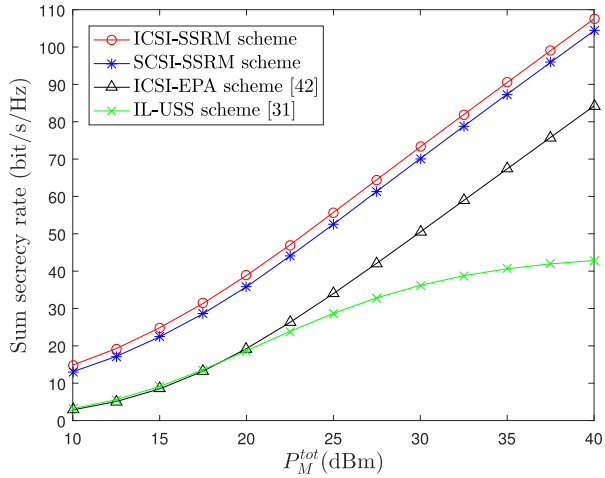

Fig. 3. Sum secrecy rate versus the transmit power of MBS P_M^{tot} for ICSI-SSRM, SCSI-SSRM, ICSI-EPA and IL-USS schemes in terms of the number of subcarriers, $N = 10$.

ICSI-SSRM and SCSI-SSRM algorithms have good convergence performance.

In Fig. 3, we present the sum secrecy rate versus the transmit power of MBS P_M^{tot} for ICSI-SSRM, SCSI-SSRM, ICSI based equal power allocation (ICSI-EPA) [42] and interference-limited underlay spectrum sharing (IL-USS) [31] schemes in terms of the number of subcarriers, $N = 10$. In ICSI-EPA and IL-USS schemes, the powers of MBS's OFDM subcarriers are equalled allocated with a given transmit power of MBS P_M^{tot}, and the corresponding fixed powers are allocated for different OFDM subcarriers of SBS, i.e., $P_{M,n}/P_{S,n} = 0.6$. As we see, the secrecy performance of proposed ICSI-SSRM, SCSI-SSRM and IL-USS schemes improves as the transmit power of MBS P_M^{tot} increases from 10 dBm to 30 dBm. This is because that increasing the transmit power of MBS results in more interference received at MU, SU and E. Meanwhile, since that the fading gains of $E(|h_{Me,n}|^2) = E(|h_{Se,n}|^2) = 1$ are higher than the fading gains of $E(|h_{Ms,n}|^2) = E(|h_{Sm,n}|^2) = 0.1$, more interference would be received at E than MU and SU. Therefore, the sum secrecy rate performance of ICSI-SSRM, SCSI-SSRM and IL-USS schemes is improved with an increasing transmit power of MBS P_M^{tot}. Moreover, as the transmit power of MBS P_M^{tot} increases beyond 30 dBm, the sum secrecy rate performance of ICSI-SSRM and SCSI-SSRM schemes continues to improve, whereas the IL-USS scheme converges to a sum secrecy rate floor. This is due to the fact that by increasing the transmit power of MBS P_M^{tot}, it results in a significant amount of mutual interference received at MU and SU in the IL-USS scheme. Thus, no improvement is obtained in the IL-USS scheme for a sufficiently high level of the transmit power. However, in ICSI-SSRM and SCSI-SSRM schemes, the SBS-MU interference is cancelled out by using a specially-designed signal at MBS, leading to a continued improvement of the sum secrecy rate with an increasing transmit power P_M^{tot}. Additionally, the proposed ICSI-SSRM and SCSI-SSRM schemes outperform the ICSI-EPA scheme in term of sum secrecy rate, which is due to the fact that our ICSI-SSRM and SCSI-SSRM schemes are proposed by optimizing power allocation of MBS and SBS across different OFDM subcarriers. Fig. 3 further demonstrates that the ICSI-SSRM scheme achieves a better sum secrecy rate performance than SCSI-SSRM strategy.

Fig. 4 illustrates the sum secrecy rate versus the number of subcarriers N for ICSI-SSRM, SCSI-SSRM, ICSI-EPA and IL-USS schemes in terms of the transmit power of MBS, $P_M^{tot} = 20$ dBm. As observed, the proposed ICSI-SSRM and SCSI-SSRM schemes outperform the ICSI-EPA and IL-USS

$$\left(\hat{P}_{M,n}^{k+1}, \hat{P}_{S,n}^{k+1}\right) = \arg \max_{P_{M,n}, P_{S,n}} \sum_{n=1}^{N} g_1(P_{M,n}, P_{S,n}) - g_2\left(\hat{P}_{M,n}^{k}, \hat{P}_{S,n}^{k}\right)$$

$$- \frac{\left(P_{M,n} - \hat{P}_{M,n}^{k}\right)|h_{Ms,n}|^2 + \left(P_{S,n} - \hat{P}_{S,n}^{k}\right)|h_{Ms,n}|^2\left(|h_{Sm,n}|^2 - \sigma_{Sm,n}^2\right)/\sigma_{Mm,n}^2}{\left[\hat{P}_{M,n}^{k}|h_{Ms,n}|^2 + \hat{P}_{S,n}^{k}|h_{Ms,n}|^2(|h_{Sm,n}|^2 - \sigma_{Sm,n}^2)/\sigma_{Mm,n}^2 + \sigma_{s,n}^2\right]\ln 2}$$

$$- \frac{2[(P_{M,n} - \hat{P}_{M,n}^{k})\sigma_{Me,n}^2 + (P_{S,n} - \hat{P}_{S,n}^{k})(\sigma_{Se,n}^2|h_{Mm,n}|^2 + \sigma_{Me,n}^2|h_{Sm,n}|^2 - \sigma_{Me,n}^2\sigma_{Sm,n}^2)/\sigma_{Mm,n}^2]}{[\hat{P}_{M,n}^{k}\sigma_{Me,n}^2 + \hat{P}_{S,n}^{k}(\sigma_{Se,n}^2|h_{Mm,n}|^2 + \sigma_{Me,n}^2|h_{Sm,n}|^2 - \sigma_{Me,n}^2\sigma_{Sm,n}^2)/\sigma_{Mm,n}^2 + \sigma_{e,n}^2]\ln 2}$$

$$\text{s.t.} \quad C1 - C2 \tag{36}$$

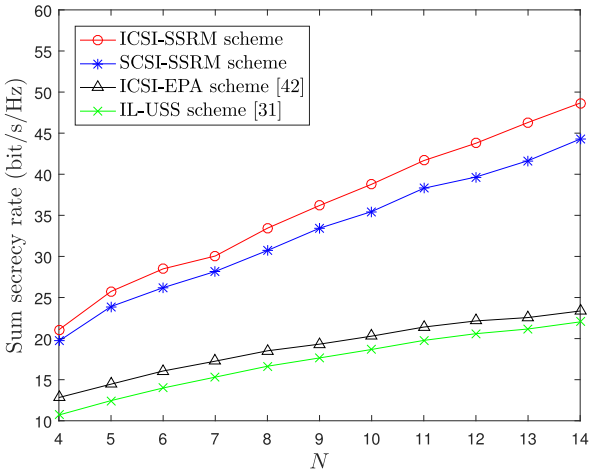

Fig. 4. Sum secrecy rate versus the number of subcarriers N for ICSI-SSRM, SCSI-SSRM, ICSI-EPA and IL-USS schemes in terms of the transmit power of MBS, $P_M^{tot} = 20$ dBm.

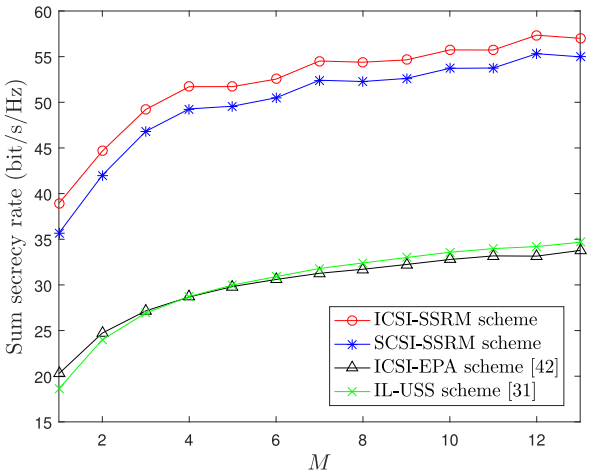

Fig. 5. Sum secrecy rate of a multi-cell heterogeneous cellular network versus the number of small cells M for ICSI-SSRM, SCSI-SSRM, ICSI-EPA and IL-USS schemes with the transmit power of MBS, $P_M^{tot} = 20$ dBm, and the number of subcarriers, $N = 10$.

methods in terms of sum secrecy rate, this further confirms the security advantage of proposed ICSI-SSRM and SCSI-SSRM schemes. Moreover, with an increasing number of subcarriers N, the sum secrecy rates of ICSI-SSRM, SCSI-SSRM, ICSI-EPA and IL-USS schemes significantly increase, which demonstrates that it is benefit to SSR by increasing the number of subcarriers N.

Fig. 5 plots the sum secrecy rate of a multi-cell heterogeneous cellular network versus the number of small cells M for ICSI-SSRM, SCSI-SSRM, ICSI-EPA and IL-USS schemes with the transmit power of MBS, $P_M^{tot} = 20$ dBm, and the number of subcarriers, $N = 10$. Here, we consider a large-scale heterogeneous cellular network with a macro cell and M small cells, where each small cell consists of a SBS and a SU. Firstly, a small cell with the best CSI of main link is selected to communicate with its associated user at each subcarrier. Thus, the best small cell selection criterion at nth subcarrier is given by $\arg\max_{m\in M} |h_{S_m s_m,n}|^2$. Then, we employ Algorithms 1 and 2 to solve the ICSI-SSRM and SCSI-SSRM problems in a large-scale heterogeneous cellular network, respectively. As shown in Fig. 5, the sum secrecy rate of the proposed ICSI-SSRM, SCSI-SSRM, ICSI-EPA and IL-USS schemes is significantly improved as the number of small cells M continues increasing. Furthermore, the proposed ICSI-SSRM strategy obtains a better sum secrecy rate performance than SCSI-SSRM, ICSI-EPA and IL-USS methods, which verifies the advantage of our proposed ICSI-SSRM scheme.

V. Conclusion

In this paper, we studied the PLS of an OFDM-based heterogeneous cellular network consisting of a macro cell and a small cell with the the existence of a common eavesdropper. An artificially designed signal was emitted at MBS to offset the interference caused by SBS and degrade the wiretap of eavesdropper. Moreover, in order to maximize the sum secrecy rate of both macro cell and small cell in an OFDM-based heterogeneous cellular network, we examined the optimization of power allocation between MBS and SBS across different OFDM subcarriers through considering the instantaneous and statistical CSI of eavesdropper. Since the proposed ICSI-SSRM and SCSI-SSRM problems are non-convex, we respectively transformed them into convex problems by employing the D.C. approach, and then presented corresponding iterative power allocation algorithms to obtain optimal solutions of the proposed ICSI-SSRM and SCSI-SSRM schemes. Finally, numerical results showed that the proposed ICSI-SSRM and SCSI-SSRM schemes obtain a higher secrecy rate than conventional power allocation schemes.

Appendix A
Derivation of (25) and (26)

According to [35], the lower bound of objective problem in (23) can be expressed as

$$\max_{P_{M,n},P_{S,n}} \sum_{n=1}^{N} C_{Mm,n} + C_{Ss,n} - \mathrm{E}[C_{Me,n}] - \mathrm{E}\,[C_{Se,n}] \quad \text{s.t.} \quad C1 - C2, \tag{A.1}$$

according to Jensen's inequality, we achieve

$$\mathrm{E}[C_{Me,n}] = \mathrm{E}[\log_2(1+\gamma_{Me,n})] \le \log_2[1+\mathrm{E}(\gamma_{Me,n})], \tag{A.2}$$

and

$$\mathrm{E}[C_{Se,n}] = \mathrm{E}[\log_2(1+\gamma_{Se,n})] \le \log_2[1+\mathrm{E}(\gamma_{Se,n})], \tag{A.3}$$

where $\mathrm{E}(\gamma_{Me,n})$ and $\mathrm{E}(\gamma_{Se,n})$ are given at (A.4) and (A.5) shown at the top of the next page, respectively. Then, following [35], when the variances of $|h_{Se,n}|^2$ and $|h_{Me,n}|^2$ are small, the $\mathrm{E}(\gamma_{Me,n})$ and $\mathrm{E}(\gamma_{Se,n})$ can be approximated into (A.6) shown at the top of the next page, and

$$\begin{aligned}\mathrm{E}(\gamma_{Me,n}) &= \mathrm{E}\left[\frac{(P_{M,n}-\sigma^2_{Sm,n}P_{S,n}/\sigma^2_{Mm,n})|h_{Me,n}|^2}{P_{S,n}(|h_{Mm,n}|^2|h_{Se,n}|^2+|h_{Sm,n}|^2|h_{Me,n}|^2)/\sigma^2_{Mm,n}+\sigma^2_{e,n}}\right]\\ &= \mathrm{E}\left[\left(P_{M,n}-\sigma^2_{Sm,n}P_{S,n}/\sigma^2_{Mm,n}\right)|h_{Me,n}|^2\right]\mathrm{E}\left[\frac{1}{P_{S,n}(|h_{Mm,n}|^2|h_{Se,n}|^2+|h_{Sm,n}|^2|h_{Me,n}|^2)/\sigma^2_{Mm,n}+\sigma^2_{e,n}}\right]\\ &= \left(P_{M,n}-\sigma^2_{Sm,n}P_{S,n}/\sigma^2_{Mm,n}\right)\sigma^2_{Me,n}\,\mathrm{E}\left[\frac{1}{P_{S,n}(|h_{Mm,n}|^2|h_{Se,n}|^2+|h_{Sm,n}|^2|h_{Me,n}|^2)/\sigma^2_{Mm,n}+\sigma^2_{e,n}}\right] \quad (A.4)\end{aligned}$$

$$\begin{aligned}\mathrm{E}(\gamma_{Se,n}) &= \mathrm{E}\left[\frac{P_{S,n}|h_{Se,n}|^2|h_{Mm,n}|^2/\sigma^2_{Mm,n}}{[P_{M,n}+\left(|h_{Sm,n}|^2-\sigma^2_{Sm,n}\right)P_{S,n}/\sigma^2_{Mm,n}]|h_{Me,n}|^2+\sigma^2_{e,n}}\right]\\ &= \mathrm{E}\left[P_{S,n}|h_{Se,n}|^2|h_{Mm,n}|^2/\sigma^2_{Mm,n}\right]\mathrm{E}\left\{\frac{1}{\left[P_{M,n}+\left(|h_{Sm,n}|^2-\sigma^2_{Sm,n}\right)P_{S,n}/\sigma^2_{Mm,n}\right]|h_{Me,n}|^2+\sigma^2_{e,n}}\right\}\\ &= P_{S,n}\sigma^2_{Se,n}|h_{Mm,n}|^2/\sigma^2_{Mm,n}\,\mathrm{E}\left\{\frac{1}{\left[P_{M,n}+\left(|h_{Sm,n}|^2-\sigma^2_{Sm,n}\right)P_{S,n}/\sigma^2_{Mm,n}\right]\sigma^2_{Me,n}+\sigma^2_{e,n}}\right\} \quad (A.5)\end{aligned}$$

$$\begin{aligned}\mathrm{E}(\gamma_{Me,n}) &\approx \frac{(P_{M,n}-\sigma^2_{Sm,n}P_{S,n}/\sigma^2_{Mm,n})\sigma^2_{Me,n}}{P_{S,n}\left(|h_{Mm,n}|^2\mathrm{E}[|h_{Se,n}|^2]+|h_{Sm,n}|^2\mathrm{E}[|h_{Me,n}|^2]\right)/\sigma^2_{Mm,n}+\sigma^2_{e,n}}\\ &= \frac{\left(P_{M,n}-\sigma^2_{Sm,n}P_{S,n}/\sigma^2_{Mm,n}\right)\sigma^2_{Me,n}}{P_{S,n}\left(|h_{Mm,n}|^2\sigma^2_{Se,n}+|h_{Sm,n}|^2\sigma^2_{Me,n}\right)/\sigma^2_{Mm,n}+\sigma^2_{e,n}} \quad (A.6)\end{aligned}$$

$$\begin{aligned}&\mathrm{E}(\gamma_{Se,n}) \approx\\ &\frac{P_{S,n}|h_{Se,n}|^2|h_{Mm,n}|^2/\sigma^2_{Mm,n}}{\left(P_{M,n}+(|h_{Sm,n}|^2-\sigma^2_{Sm,n})P_{S,n}/\sigma^2_{Mm,n}\right)\mathrm{E}\left[|h_{Me,n}|^2\right]+\sigma^2_{e,n}}\\ &= \frac{P_{S,n}\sigma^2_{Se,n}|h_{Mm,n}|^2/\sigma^2_{Mm,n}}{\left[P_{M,n}+(|h_{Sm,n}|^2-\sigma^2_{Sm,n})P_{S,n}/\sigma^2_{Mm,n}\right]\sigma^2_{Me,n}+\sigma^2_{e,n}}. \quad (A.7)\end{aligned}$$

Appendix B
Proof of Lemma

It is clear that the object functions in (20) and (27) are positive linear combinations of logarithm functions $h(x,y)=\ln(a_1x+b_1y+c_1)-\ln(a_2x+b_2y+c_2)$, where a_1, a_2, b_1, b_2, c_1 and c_2 are constants, x and y are nonnegative variables. Following [43], the concavity and convexity of a two-dimensional function relies on concave-convex characteristic of its restriction to any line. Thus, we can achieve

$$\begin{aligned}h(x) &= h(x,y)|_{y=\alpha x+\beta}\\ &= \ln\left[a_1x+b_1(\alpha x+\beta)+c_1\right]-\ln\left[a_2x+b_2(\alpha x+\beta)+c_2\right]\\ &= \ln\left[(a_1+b_1\alpha)x+b_1\beta+c_1\right]-\ln\left[(a_2+b_2\alpha)x+b_2\beta+c_2\right], \quad (B.1)\end{aligned}$$

Then, first and second order derivatives of (B.1) can respectively expressed as

$$h'(x)=\frac{a_1+b_1\alpha}{(a_1+b_1\alpha)x+b_1\beta+c_1}-\frac{a_2+b_2\alpha}{(a_2+b_2\alpha)x+b_2\beta+c_2}, \quad (B.2)$$

and

$$\begin{aligned}&h''(x)\\ &= \frac{-(a_1+b_1\alpha)^2}{\left[(a_1+b_1\alpha)x+b_1\beta+c_1\right]^2}+\frac{(a_2+b_2\alpha)^2}{\left[(a_2+b_2\alpha)x+b_2\beta+c_2\right]^2}, \quad (B.3)\end{aligned}$$

from which, the positive and negative characteristics of $h''(x)$ depend on specific values of a_1, a_2, b_1, b_2, c_1, c_2, α, β and x, which means that $h(x)$ is non-convex. We can conclude that $h(x,y)$ is non-convex, namely, the object functions in (20) and (27) are non-convex.

Appendix C
Proof of Convergence

It can be observed that the principle of iterative optimal power allocation algorithms for ICSI-SSRM and SCSI-SSRM schemes are same, thus we only need to prove the convergence of the ICSI-SSRM algorithm. From (30), we have the inequation (C.1). Then, following the iterative procedure in (32), we obtain the formula (C.2). Combining (C.1) and (C.2), we further achieve (C.3). From (C.3), we obvious that as the iterative numbers

$$
\begin{aligned}
&f_2\big(\tilde{P}_{M,n}^{k+1},\tilde{P}_{S,n}^{k+1}\big)\\
&\quad\le f_2\big(\tilde{P}_{M,n}^{k},\tilde{P}_{S,n}^{k}\big)+\frac{\big(\tilde{P}_{M,n}^{k+1}-\tilde{P}_{M,n}^{k}\big)|h_{Ms,n}|^2+\big(\tilde{P}_{S,n}^{k+1}-\tilde{P}_{S,n}^{k}\big)|h_{Ms,n}|^2\big(|h_{Sm,n}|^2-\sigma_{Sm,n}^2\big)/\sigma_{Mm,n}^2}{\Big[\tilde{P}_{M,n}^{k}|h_{Ms,n}|^2+\tilde{P}_{S,n}^{k}|h_{Ms,n}|^2\big(|h_{Sm,n}|^2-\sigma_{Sm,n}^2\big)/\sigma_{Mm,n}^2+\sigma_{s,n}^2\Big]\ln 2}\\
&\qquad+\frac{2\Big[\big(\tilde{P}_{M,n}^{k+1}-\tilde{P}_{M,n}^{k}\big)|h_{Me,n}|^2+\big(\tilde{P}_{S,n}^{k+1}-\tilde{P}_{S,n}^{k}\big)\big(|h_{Se,n}|^2|h_{Mm,n}|^2+|h_{Me,n}|^2|h_{Sm,n}|^2-|h_{Me,n}|^2\sigma_{Sm,n}^2\big)/\sigma_{Mm,n}^2\Big]}{\Big[\tilde{P}_{M,n}^{k}|h_{Me,n}|^2+\tilde{P}_{S,n}^{k}\big(|h_{Se,n}|^2|h_{Mm,n}|^2+|h_{Me,n}|^2|h_{Sm,n}|^2-|h_{Me,n}|^2\sigma_{Sm,n}^2\big)/\sigma_{Mm,n}^2+\sigma_{e,n}^2\Big]\ln 2}
\end{aligned}
\tag{C.1}
$$

$$
\begin{aligned}
&\sum_{n=1}^{N}f_1\big(\tilde{P}_{M,n}^{k+1},\tilde{P}_{S,n}^{k+1}\big)-f_2\big(\tilde{P}_{M,n}^{k},\tilde{P}_{S,n}^{k}\big)-\frac{\big(\tilde{P}_{M,n}^{k+1}-\tilde{P}_{M,n}^{k}\big)|h_{Ms,n}|^2+\big(\tilde{P}_{S,n}^{k+1}-\tilde{P}_{S,n}^{k}\big)|h_{Ms,n}|^2\big(|h_{Sm,n}|^2-\sigma_{Sm,n}^2\big)/\sigma_{Mm,n}^2}{\Big[\tilde{P}_{M,n}^{k}|h_{Ms,n}|^2+\tilde{P}_{S,n}^{k}|h_{Ms,n}|^2\Big(|h_{Sm,n}|^2-\sigma_{Sm,n}^2\Big)/\sigma_{Mm,n}^2+\sigma_{s,n}^2\Big]\ln 2}\\
&\quad-\frac{2\Big[\big(\tilde{P}_{M,n}^{k+1}-\tilde{P}_{M,n}^{k}\big)|h_{Me,n}|^2+\big(\tilde{P}_{S,n}^{k+1}-\tilde{P}_{S,n}^{k}\big)\big(|h_{Se,n}|^2|h_{Mm,n}|^2+|h_{Me,n}|^2|h_{Sm,n}|^2-|h_{Me,n}|^2\sigma_{Sm,n}^2\big)/\sigma_{Mm,n}^2\Big]}{\Big[\tilde{P}_{M,n}^{k}|h_{Me,n}|^2+\tilde{P}_{S,n}^{k}\big(|h_{Se,n}|^2|h_{Mm,n}|^2+|h_{Me,n}|^2|h_{Sm,n}|^2-|h_{Me,n}|^2\sigma_{Sm,n}^2\big)/\sigma_{Mm,n}^2+\sigma_{e,n}^2\Big]\ln 2}\\
&=\max_{P_{M,n},P_{S,n}}\sum_{n=1}^{N}f_1(P_{M,n},P_{S,n})-f_2\big(\tilde{P}_{M,n}^{k},\tilde{P}_{S,n}^{k}\big)-\frac{\big(P_{M,n}-\tilde{P}_{M,n}^{k}\big)|h_{Ms,n}|^2+\big(P_{S,n}-\tilde{P}_{S,n}^{k}\big)|h_{Ms,n}|^2\big(|h_{Sm,n}|^2-\sigma_{Sm,n}^2\big)/\sigma_{Mm,n}^2}{\Big[\tilde{P}_{M,n}^{k}|h_{Ms,n}|^2+\tilde{P}_{S,n}^{k}|h_{Ms,n}|^2\big(|h_{Sm,n}|^2-\sigma_{Sm,n}^2\big)/\sigma_{Mm,n}^2+\sigma_{s,n}^2\Big]\ln 2}\\
&\quad-\frac{2\Big[\big(P_{M,n}-\tilde{P}_{M,n}^{k}\big)|h_{Me,n}|^2+\big(P_{S,n}-\tilde{P}_{S,n}^{k}\big)\big(|h_{Se,n}|^2|h_{Mm,n}|^2+|h_{Me,n}|^2|h_{Sm,n}|^2-|h_{Me,n}|^2\sigma_{Sm,n}^2\big)/\sigma_{Mm,n}^2\Big]}{\Big[\tilde{P}_{M,n}^{k}|h_{Me,n}|^2+\tilde{P}_{S,n}^{k}(|h_{Se,n}|^2|h_{Mm,n}|^2+|h_{Me,n}|^2|h_{Sm,n}|^2-|h_{Me,n}|^2\sigma_{Sm,n}^2)/\sigma_{Mm,n}^2+\sigma_{e,n}^2\Big]\ln 2}\\
&\ge\sum_{n=1}^{N}f_1\big(\tilde{P}_{M,n}^{k},\tilde{P}_{S,n}^{k}\big)-f_2\big(\tilde{P}_{M,n}^{k},\tilde{P}_{S,n}^{k}\big)
\end{aligned}
\tag{C.2}
$$

$$
\begin{aligned}
&\sum_{n=1}^{N}f_1\big(\tilde{P}_{M,n}^{k+1},\tilde{P}_{S,n}^{k+1}\big)-f_2\big(\tilde{P}_{M,n}^{k+1},\tilde{P}_{S,n}^{k+1}\big)\\
&\quad\ge\sum_{n=1}^{N}f_1\big(\tilde{P}_{M,n}^{k+1},\tilde{P}_{S,n}^{k+1}\big)-f_2\big(\tilde{P}_{M,n}^{k},\tilde{P}_{S,n}^{k}\big)-\frac{\big(\tilde{P}_{M,n}^{k+1}-\tilde{P}_{M,n}^{k}\big)|h_{Ms,n}|^2+\big(\tilde{P}_{S,n}^{k+1}-\tilde{P}_{S,n}^{k}\big)|h_{Ms,n}|^2\big(|h_{Sm,n}|^2-\sigma_{Sm,n}^2\big)/\sigma_{Mm,n}^2}{\Big[\tilde{P}_{M,n}^{k}|h_{Ms,n}|^2+\tilde{P}_{S,n}^{k}|h_{Ms,n}|^2\Big(|h_{Sm,n}|^2-\sigma_{Sm,n}^2\Big)/\sigma_{Mm,n}^2+\sigma_{s,n}^2\Big]\ln 2}\\
&\qquad-\frac{2\Big[\big(\tilde{P}_{M,n}^{k+1}-\tilde{P}_{M,n}^{k}\big)|h_{Me,n}|^2+\big(\tilde{P}_{S,n}^{k+1}-\tilde{P}_{S,n}^{k}\big)\big(|h_{Se,n}|^2|h_{Mm,n}|^2+|h_{Me,n}|^2|h_{Sm,n}|^2-|h_{Me,n}|^2\sigma_{Sm,n}^2\big)/\sigma_{Mm,n}^2\Big]}{\Big[\tilde{P}_{M,n}^{k}|h_{Me,n}|^2+\tilde{P}_{S,n}^{k}\big(|h_{Se,n}|^2|h_{Mm,n}|^2+|h_{Me,n}|^2|h_{Sm,n}|^2-|h_{Me,n}|^2\sigma_{Sm,n}^2\big)/\sigma_{Mm,n}^2+\sigma_{e,n}^2\Big]\ln 2}\\
&\quad\ge\sum_{n=1}^{N}f_1\big(\tilde{P}_{M,n}^{k},\tilde{P}_{S,n}^{k}\big)-f_2\big(\tilde{P}_{M,n}^{k},\tilde{P}_{S,n}^{k}\big)
\end{aligned}
\tag{C.3}
$$

$$
\begin{aligned}
&\sum_{n=1}^{N}C_{Mm,n}-C_{Me,n}+C_{Ss,n}-C_{Se,n}\\
&\quad\le\sum_{n=1}^{N}\log_2\left[1+\frac{\big(P_{M,n}-\sigma_{Sm,n}^2P_{S,n}/\sigma_{Mm,n}^2\big)|h_{Mm,n}|^2}{\sigma_{m,n}^2}\right]\\
&\qquad+\log_2\left[1+\frac{P_{S,n}|h_{Ss,n}|^2|h_{Mm,n}|^2/\sigma_{Mm,n}^2}{\big(P_{M,n}+(|h_{Sm,n}|^2-\sigma_{Sm,n}^2)P_{S,n}/\sigma_{Mm,n}^2\big)|h_{Ms,n}|^2+\sigma_{s,n}^2}\right]\\
&\quad\le\sum_{n=1}^{N}\frac{\big(P_{M,n}-\sigma_{Sm,n}^2P_{S,n}/\sigma_{Mm,n}^2\big)|h_{Mm,n}|^2}{\sigma_{m,n}^2\ln 2}+\frac{P_{S,n}|h_{Ss,n}|^2|h_{Mm,n}|^2/\sigma_{Mm,n}^2}{\Big\{\Big[P_{M,n}+(|h_{Sm,n}|^2-\sigma_{Sm,n}^2)P_{S,n}/\sigma_{Mm,n}^2\Big]|h_{Ms,n}|^2+\sigma_{s,n}^2\Big\}\ln 2}\\
&\quad\le\sum_{n=1}^{N}\frac{P_{M,n}|h_{Mm,n}|^2}{\sigma_{m,n}^2\ln 2}+\frac{P_{S,n}|h_{Ss,n}|^2|h_{Mm,n}|^2/\sigma_{Mm,n}^2}{\sigma_{s,n}^2\ln 2}\\
&\quad\le\frac{P_M^{tot}\max\big(|h_{Mm,n}|^2\big)}{\min(\sigma_{m,n}^2)\ln 2}+\frac{P_S^{tot}\max\big(|h_{Ss,n}|^2|h_{Mm,n}|^2\big)}{min\big(\sigma_{s,n}^2\sigma_{Mm,n}^2\big)\ln 2}
\end{aligned}
\tag{C.4}
$$

increase, the proposed iterative procedure is monotonically non-decreasing. In addition, due to the fact that $\sum_{n=1}^{N} P_{M,n} = P_M^{tot}$, $\sum_{n=1}^{N} P_{S,n} = P_S^{tot}$ and for $\forall x > -1$, $\log_2(1+x) \leq x/\ln 2$ as well as $0 \leq \sigma_{Sm,n}^2 P_{S,n}/\sigma_{Mm,n}^2 \leq P_{M,n}$, the upper bound of the object function (20) can be given by (C.4). Then, combining (C.3) and (C.4), we can ensure that the iterative procedure will convergence to the optimal solutions of (20).

REFERENCES

[1] G. Ding *et al.*, "Spectrum inference in cognitive radio networks: Algorithms and applications," *IEEE Commun. Surv. Tuts.*, vol. 20, no. 1, pp. 150–182, Jan.–Mar. 2018.

[2] W. Sun and J. Liu, "2-to-M coordinated multipoint-based uplink transmission in ultra-dense cellular networks," *IEEE Trans. Wireless Commun.*, vol. 17, no. 12, pp. 8342–8356, Dec. 2018.

[3] Y. Zou, "Physical-layer security for spectrum sharing systems," *IEEE Trans. Wireless Commun.*, vol. 16, no. 2, pp. 1319–1329, Feb. 2017.

[4] A. Agustin *et al.*, "Efficient use of paired spectrum bands through TDD small cell deployments," *IEEE Commun. Mag.*, vol. 55, no. 9, pp. 210–217, Sep. 2017.

[5] G. P. Koudouridis and P. Soldati, "Spectrum and network density management in 5G ultra-dense networks," *IEEE Wireless Commun.*, vol. 24, no. 5, pp. 30–37, Oct. 2017.

[6] M. Sheng, J. Wen, J. Li, B. Liang, and X. Wang, "Performance analysis of heterogeneous cellular networks with HARQ under correlated interference," *IEEE Trans. Wireless Commun.*, vol. 16, no. 12, pp. 8377–8389, Dec. 2017.

[7] J. Jia, Y. Deng, J. Chen, A. H. Aghvami, and A. Nallanathan, "Achieving high availability in heterogeneous cellular networks via spectrum aggregation," *IEEE Trans. Veh. Technol.*, vol. 66, no. 11, pp. 10156–10169, Nov. 2017.

[8] V. Chandrasekhar, J. G. Andrews, and A. Gatherer, "Femtocell networks: A survey," *IEEE Commun. Mag.*, vol. 46, no. 9, pp. 59–67, Sep. 2008.

[9] E. Turgut and M. C. Gursoy, "Coverage in heterogeneous downlink millimeter wave cellular networks," *IEEE Trans. Commun.*, vol. 65, no. 10, pp. 4463–4477, Oct. 2017.

[10] J. Garca-Morales, G. Femenias, and F. Riera-Palou, "Analysis and optimization of FFR-aided OFDMA-based heterogeneous cellular networks," *IEEE Access*, vol. 4, pp. 5111–5127, Aug. 2016.

[11] H. A. Shah and I. Koo, "A novel physical layer security scheme in OFDM-based cognitive radio networks," *IEEE Access*, vol. 6, pp. 29486–29498, Jun. 2018.

[12] J. Dai, J. Liu, Y. Shi, S. Zhang, and J. Ma, "Analytical modeling of resource allocation in D2D overlaying multiple-hop multi-channel uplink cellular networks," *IEEE Trans. Veh. Technol.*, vol. 66, no. 8, pp. 6633–6644, Aug. 2017.

[13] Z. Liu, J. Liu, Y. Zeng, and J. Ma, "Covert wireless communications in IoT: Hiding information in interference," *IEEE Wireless Commun. Mag.*, vol. 25, no. 6, pp. 46–52, Dec. 2018.

[14] D. Wu, Q. Wu, Y. Xu, J. Jing, and Z. Qin, "QoE-based distributed multichannel allocation in 5G heterogeneous cellular networks: A matching-coalitional game solution," *IEEE Access*, vol. 5, pp. 61–71, Sep. 2017.

[15] N. Zhao, F. R. Yu, M. Li, Q. Yan, and V. C. M. Leung, "Physical layer security issues in interference-alignment-based wireless networks," *IEEE Commun. Mag.*, vol. 54, no. 8, pp. 162–168, Aug. 2016.

[16] F. J. Martin-Vega, G. Gomez, M. C. Aguayo-Torres, and M. Di Renzo, "Analytical modeling of interference aware power control for the uplink of heterogeneous cellular networks," *IEEE Trans. Wireless Commun.*, vol. 15, no. 10, pp. 6742–6757, Oct. 2016.

[17] Z. H. Abbas, F. Muhammad, and L. Jiao, "Analysis of load balancing and interference management in heterogeneous cellular networks," *IEEE Access*, vol. 5, pp. 14690–14705, Jul. 2017.

[18] Y. Zou, J. Zhu, X. Wang, and L. Hanzo, "A survey on wireless security: Technical challenges, recent advances and future trends," *Proc. IEEE*, vol. 104, no. 9, pp. 1727–1765, Sep. 2016.

[19] J. Zhu and Y. Zou, "Cognitive network cooperation for green cellular networks," *IEEE Access*, vol. 4, pp. 849–857, Mar. 2016.

[20] M. Ku and J. Lai, "Joint beamforming and resource allocation for wireless-powered device-to-device communications in cellular networks," *IEEE Trans. Wireless Commun.*, vol. 16, no. 11, pp. 7290–7304, Nov. 2017.

[21] Y. Zou, J. Zhu, X. Li, and L. Hanzo, "Relay selection for wireless communications against eavesdropping: A security-reliability trade-off perspective," *IEEE Netw.*, vol. 30, no. 5, pp. 74–79, Oct. 2016.

[22] B. Wang and P. Mu, "Artificial noise-aided secure multicasting design under secrecy outage constraint," *IEEE Trans. Commun.*, vol. 65, no. 12, pp. 5401–5414, Dec. 2017.

[23] J. Liu, Z. Liu, Y. Zeng, and J. Ma, "Cooperative jammer placement for physical layer security enhancement," *IEEE Netw. Mag.*, vol. 30, no. 6, pp. 56–61, Dec. 2016.

[24] H. Wu, X. Tao, Z. Han, N. Li, and J. Xu, "Secure transmission in MISOME wiretap channel with multiple assisting jammers: Maximum secrecy rate and optimal power allocation," *IEEE Trans. Commun.*, vol. 65, no. 2, pp. 775–789, Feb. 2017.

[25] J. Liu, H. Nishiyama, N. Kato, and J. Guo, "On the outage probability of device-to-device-communication-enabled multichannel cellular networks: An RSS-threshold-based perspective," *IEEE J. Sel. Areas Commun.*, vol. 34, no. 1, pp. 163–175, Jan. 2016.

[26] J. Liu, N. Kato, J. Ma, and N. Kadowaki, "Device-to-device communication in LTE-advanced networks: A survey," *IEEE Commun. Surv. Tuts.*, vol. 17, no. 4, pp. 1923–1940, Nov. 2015.

[27] J. Liu, S. Zhang, N. Kato, H. Ujikawa, and K. Suzuki, "Device-to-device communications for enhancing quality of experience in software defined multi-tier LTE-A networks," *IEEE Netw. Mag.*, vol. 29, no. 4, pp. 46–52, Jul. 2015.

[28] J. Liu, Y. Kawamoto, H. Nishiyama, N. Kato, and N. Kadowaki, "Device-to-device communications achieve efficient load balancing in LTE-advanced networks," *IEEE Wireless Commun. Mag.*, vol. 21, no. 2, pp. 57–65, Apr. 2014.

[29] H. Wang, T. Zheng, J. Yuan, D. Towsley, and M. H. Lee, "Physical layer security in heterogeneous cellular networks," *IEEE Trans. Commun.*, vol. 64, no. 3, pp. 1204–1219, Mar. 2016.

[30] W. Tang, S. Feng, Y. Ding, and Y. Liu, "Physical layer security in heterogeneous networks with jammer selection and full-duplex users," *IEEE Trans. Wireless Commun.*, vol. 16, no. 12, pp. 7982–7995, Dec. 2017.

[31] Y. Zou, "Intelligent interference exploitation for heterogeneous cellular networks against eavesdropping," *IEEE J. Sel. Areas Commun.*, vol. 36, no. 7, pp. 1453–1464, Jul. 2018.

[32] Y. Zou, M. Sun, J. Zhu, and H. Guo, "Security-reliability tradeoff for distributed antenna systems in heterogeneous cellular networks," *IEEE Trans. Wireless Commun.*, vol. 17, no. 12, pp. 8444–8456, Dec. 2018.

[33] S. Li, P. J. Smith, P. A. Dmochowski, and J. Yin, "Analysis of analog and digital MRC for distributed and centralized MU-MIMO systems," *IEEE Trans. Veh. Technol.*, vol. 68, no. 2, pp. 1948–1952, Feb. 2019.

[34] G. Wang, Q. Liu, R. He, and F. Gao, "Acquisition of channel state information in heterogeneous cloud radio access networks: Challenges and research directions," *IEEE Wireless Commun.*, vol. 22, no. 3, pp. 100–107, Jun. 2015.

[35] H. Guo, Z. Yang, L. Zhang, J. Zhu, and Y. Zou, "Power-constrained secrecy rate maximization for joint relay and jammer selection assisted wireless networks," *IEEE Trans. Commun.*, vol. 65, no. 5, pp. 2180–2193, May 2017.

[36] Z. Chu, H. Xing, M. Johnston, and S. Le Goff, "Secrecy rate optimizations for a MISO secrecy channel with multiple multiantenna eavesdroppers," *IEEE Trans. Wireless Commun.*, vol. 15, no. 1, pp. 283–297, Jan. 2016.

[37] C. Jiang *et al.*, "Cross-layer optimization for multi-hop wireless networks with successive interference cancellation," *IEEE Trans. Wireless Commun.*, vol. 15, no. 8, pp. 5819–5831, Aug. 2016.

[38] H. H. Kha, H. D. Tuan, and H. H. Nguyen, "Fast global optimal power allocation in wireless networks by local DC programming," *IEEE Tans. Wireless Commun.*, vol. 11, no. 2, pp. 510–515, Feb. 2012.

[39] M. Grant and S. Boyd, "CVX: Matlab software for disciplined convex programming, version 2.1," Mar. 2014. [Online.] Available: http://cvxr.com/cvx

[40] Z.-Q. Luo, W.-K. Ma, A. M.-C. So, Y. Ye, and S. Zhang, "Semidefinite relaxation of quadratic optimization problems," *IEEE Signal Process. Mag.*, vol. 27, no. 3, pp. 20–34, May 2010.

[41] J. Ouyang, M. Lin, Y. Zou, W.-P. Zhu, and D. Massicotte, "Secrecy energy efficiency maximization in cognitive radio networks," *IEEE Access*, vol. 5, pp. 2641–2650, Feb. 2017.

[42] M. R. Abedi, N. Mokari, M. R. Javan, and H. Yanikomeroglu, "Secure communication in OFDMA-based cognitive radio networks: An incentivized secondary network coexistence approach," *IEEE Trans. Veh. Technol.*, vol. 66, no. 2, pp. 1171–1185, Feb. 2017.

[43] W. Yu and J. M. Cioffi, "FDMA capacity of Gaussian multiple-access channels with ISI," *IEEE Trans. Commun.*, vol. 50, no. 1, pp. 102–111, Jan. 2002.

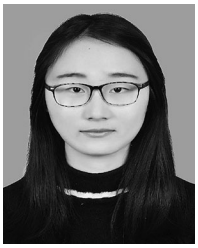

Yuhan Jiang received the B.Eng. degree in communication engineering from Nantong University, Nantong, China, in July 2016. She is currently working toward the Ph.D. degree in signal and information processing with the Nanjing University of Posts and Telecommunications, Nanjing, China. Her research interests include cognitive radio, physical-layer security, and green communications.

Yulong Zou (Senior Member, IEEE) received the B.Eng. degree in information engineering from the Nanjing University of Posts and Telecommunications (NUPT), Nanjing, China, in July 2006, the Ph.D. degree in electrical engineering from the Stevens Institute of Technology, Hoboken, NJ, USA, in May 2012, and the Ph.D. degree in signal and information processing from NUPT in July 2012. He is currently a Full Professor and Doctoral Supervisor with NUPT. He was the recipient of the 9th IEEE Communications Society Asia-Pacific Best Young Researcher in 2014 and was a co-recipient of the Best Paper Award at the 80th IEEE Vehicular Technology Conference in 2014. He was an Editor of the IEEE COMMUNICATIONS SURVEYS & TUTORIALS, IEEE COMMUNICATIONS LETTERS, *EURASIP Journal on Advances in Signal Processing*, *IET Communications*, and *China Communications*. In addition, he was a TPC Member for various IEEE sponsored conferences, e.g., IEEE ICC/GLOBECOM/WCNC/VTC/ICCC, etc.

Haiyan Guo received the B.Eng. and Ph.D. degrees in signal and information processing from the Nanjing University of Posts and Telecommunications (NUPT), Nanjing, China, in 2005 and 2011, respectively. From 2013 to 2014, she was a Postdoctoral Research Fellow with Southeast University. She is currently an Assistant Professor with NUPT. Her research interests include physical-layer security, energy harvesting, and speech signal processing.

Jia Zhu received the B.Eng. degree in computer science and technology from the Hohai University, Nanjing, China, in July 2005, and the Ph.D. degree in signal and information processing from the Nanjing University of Posts and Telecommunications (NUPT), Nanjing, China, in April 2010. She is currently a Full Professor with NUPT. From June 2010 to June 2012, she was a Postdoctoral Research Fellow with the Stevens Institute of Technology, Hoboken, NJ, USA. Since November 2012, she has been a Full-Time Faculty Member with the Telecommunication and Information School, NUPT. Her general research interests include the cognitive radio, physical-layer security, and communications theory.

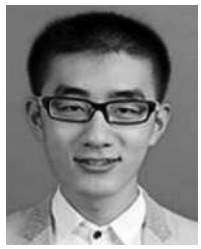

Jiahao Gu is currently working toward the B.Eng. degree in communication engineering with the Nanjing University of Posts and Telecommunications, Nanjing, China. His research interests include cognitive radio, physical-layer security, and machine learning in communications.